Dynamical collision network in granular gases

J. Ignacio Alvarez-Hamelin[1] and Andrea Puglisi[2]
[1]*CONICET and Facultad de Ingeniería, Universidad de Buenos Aires, Paseo Colón 850, C1063ACV Buenos Aires, Argentina*
[2]*Dipartimento di Fisica, Università La Sapienza, p.le Aldo Moro 2, 00185 Roma, Italy*
(Received 13 September 2006; revised manuscript received 26 February 2007; published 2 May 2007)

We address the problem of recollisions in cooling granular gases. To this aim, we dynamically construct the interaction network in a granular gas, using the sequence of collisions collected in an event driven simulation of inelastic hard disks from time 0 until time t. The network is decomposed into its k-core structure: particles in a core of index k have collided at least k times with other particles in the same core. The difference between cores $k+1$ and k is the so-called k-shell, and the set of all shells is a complete and nonoverlapping decomposition of the system. Because of energy dissipation, the gas cools down: its initial spatially homogeneous dynamics, characterized by the Haff law, i.e., a t^{-2} energy decay, is unstable toward a strongly inhomogeneous phase with clusters and vortices, where energy decays as t^{-1}. The clear transition between those two phases appears in the evolution of the k-shells structure in the collision network. In the homogeneous state the k-shell structure evolves as in a growing network with a fixed number of vertices and randomly added links: the shell distribution is strongly peaked around the most populated shell, which has an index $k_{\max} \sim 0.9\langle d\rangle$ with $\langle d\rangle$ the average number of collisions experienced by a particle. During the final nonhomogeneous state a growing fraction of collisions is concentrated in small, almost closed, *communities* of particles: $k_{\max}$ is no more linear in $\langle d\rangle$ and the distribution of shells becomes extremely large developing a power-law tail $\sim k^{-3}$ for high shell indexes. We conclude proposing a simple algorithm to build a correlated random network that reproduces, with few essential ingredients, the whole observed phenomenology, including the t^{-1} energy decay. It consists of two kinds of collisions (links): single random collisions with any other particle and long chains of recollisions with only previously encountered particles. The algorithm disregards the exact spatial arrangement of clusters, suggesting that the observed stringlike structures are not essential to determine the statistics of recollisions and the energy decay.

DOI: 10.1103/PhysRevE.75.051302 PACS number(s): 45.70.−n, 51.10.+y, 89.75.Hc

I. INTRODUCTION

The study of dilute granular materials [1], as well as of many other particle systems lacking an equilibrium description (glass forming liquids in their nonequilibrium regime [2], for instance), requires the use of appropriate tools, models, and paradigms in order to simplify the picture and gain new insights. The introduction of the free inelastic hard spheres model has been of fundamental relevance for the rigorous foundation of granular kinetic theory and hydrodynamics [3]. The model consists of a gas of N hard spheres in a volume V, with inelastic collisions modeling the macroscopic nature of grains: part of the energy of the relative motion between two colliding grains is irreversibly dissipated into heat. Such simple generalization of the hard sphere model leads to dramatic consequences: the gas performs a nonstationary dynamics, cooling down and evolving toward a final state of thermal death. Moreover, in large enough systems a homogeneous granular gas is unstable toward the formation of vortices and clusters of closely packed grains.

A satisfying description of the late dynamics of the gas, after the onset of strong inhomogeneity, is still lacking. Coarse-grained descriptions in terms of hydrodynamic fields are made difficult by an apparently general lack of separation between microscopic and macroscopic scales [4,5]. Velocity or density structure factors, usually difficult to measure because of rapid temporal evolution, indicate a generic growth of structures but are insufficient to appreciate the rich kinetic behavior at the level of small groups of grains. Analogies with percolation transitions, Burgers models, or two-dimensional (2D) turbulence have been proposed, sometimes on the mere basis of phenomenological similitudes.

In front of the openness of this problem, we propose a method of analysis, borrowed to the graph's theory, the so-called k-core analysis [6–8]: a k-core is the maximum subgraph containing only nodes with at least k links in the same subgraph. Very recently, the theory of k-cores has proven to be useful in defining a possible universality class for the dynamical glass transition, the bootstrap (also called "jamming") percolation [9]. In simple models of glass forming liquids, at finite temperature and above a critical value of the tunable average density, a jammed giant component in the k-core subset of the contact network (defined in a specific way) percolates the system, marking a breaking of ergodicity. Even if these works have been of some inspiration to us, we stress that our study addresses a different phenomenology and applies the analysis of graphs in a substantially different way. Therefore we do not claim any analogy between the dynamical breaking of the homogeneous cooling state of a granular gas and the jamming percolation or any other proposed glass transition scenario.

Our proposal is to dynamically construct a graph by linking two nodes (particles) each time a collision happens: the resulting graph grows with time and the average number of links per node is equal to two times the average number of collisions per particle. The decomposition of the interaction network into a hierarchy of cores of increasing degree of self-interaction will prove to be a powerful tool to distin-

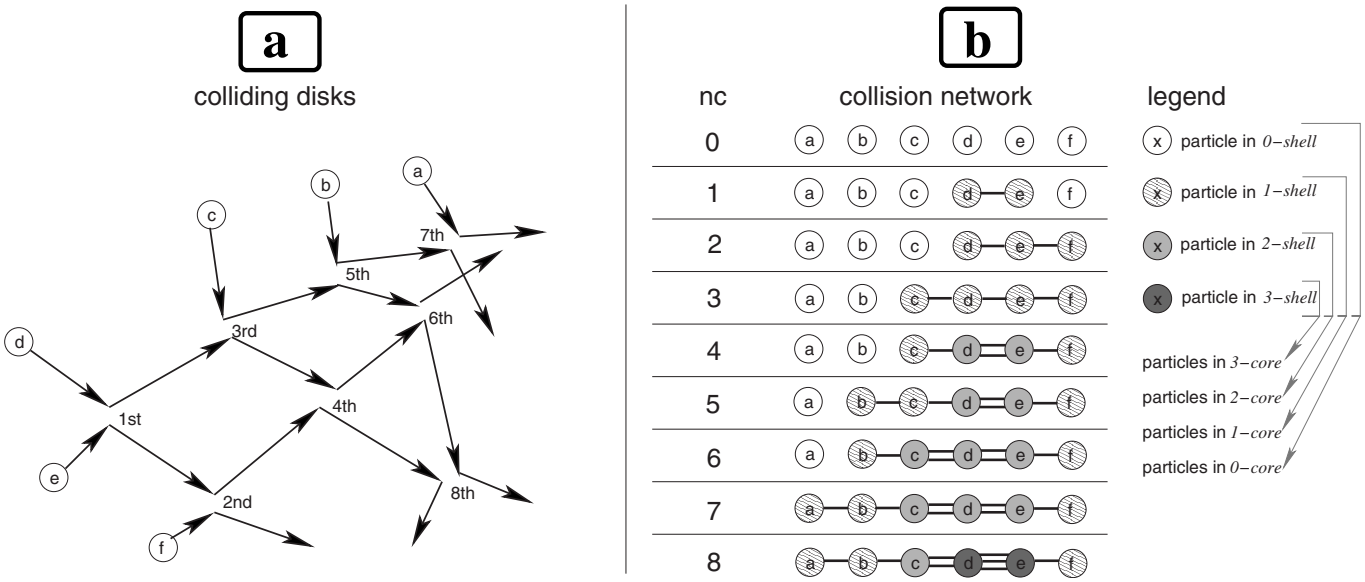

FIG. 1. Evolution of the network of collisions for a system of six particles. (a) The ordered sequence of collisions. (b) Collision network at each time step, where *nc* is the number of realized collisions. All particles are in the core of index 0. Particles not appearing in higher cores are also in the shell of index 0. In general a k-core has all the particles with shell index $\geqslant k$.

guish between particles in the solidlike phase from those in the fluidlike phase. The sequence of collisions in the nonhomogeneous state is in fact dominated by repeated impacts among grains trapped into sorts of self-sustained cages with very small escape probabilities. Such cages can be thought of as almost closed *communities* in an interaction network. Strongly dissipating collisions, on the other side, are mostly concentrated outside of those cages, in the periphery of clusters, and involve particles which still have a certain degree of mobility.

More specifically, the k-core decomposition of the collision network appears as the natural characterization of the violation of molecular chaos. In an ideal gas, i.e., a gas satisfying the molecular chaos assumption, a grain never collides with another grain that is connected (through collisions) to its own previous history. In terms of graphs, true molecular chaos is equivalent to the following statement: the collision network is a tree, and therefore all the cores of index larger than 1 are empty. The minimal mechanism of molecular chaos breaking is that of *rings collisions*, which appear as loops in the collision graph, i.e., the simplest structures in cores of index 2. An example of dynamical collision network, with trees and loops, is given in Fig. 1. Cores of high degrees, i.e., systematic violations of molecular chaos, appear naturally in any finite system, even with purely random collisions. We will focus on the difference between effects on the k-core decomposition due to finite-size and those really induced by inelasticity.

In Sec. II a description of the model of inelastic hard disks and of its known regimes will be given. The construction of the dynamical collision network will be explained in Sec. III. In Sec. IV we will show numerical results for the homogeneous state, while the nonhomogeneous state will be discussed in Sec. V. In Sec. VI we discuss a model of random correlated collisions that reproduces the main features observed in a nonhomogeneous granular gas. A discussion with conclusions and perspectives will come in Sec. VII.

II. THE GRANULAR GAS OF INELASTIC HARD SPHERES

One of the simplest models of granular gas is the gas of free inelastic hard objects (rods, disks, or spheres, depending on the dimensionality) with constant coefficient of restitution. We restrict the discussion to $D=2$ dimensions, considering an assembly of N inelastic hard disks of diameter 1 and mass 1 in a box of volume $V=L\times L$ with periodic boundary conditions. Between collisions each particle moves freely. When two particles i and j collide their velocities change from $\mathbf{v}_i,\mathbf{v}_j$ to $\mathbf{v}_i',\mathbf{v}_j'$, using the following rule:

$$\mathbf{v}_{i(j)}' = \mathbf{v}_{i(j)} - \frac{1+\alpha}{2}[(\mathbf{v}_{i(j)} - \mathbf{v}_{j(i)})\cdot\hat{\boldsymbol{\sigma}}]\hat{\boldsymbol{\sigma}}, \tag{1}$$

where $\alpha\in[0,1]$ is the restitution coefficient, while $\hat{\boldsymbol{\sigma}}$ is the unity vector joining the centers of the two particles.

This model is widely used in the theoretical work on granular gases, conveying usefulness and simplicity: it reproduces the main features of real dilute granular experiments, allows fast event driven simulations, and is prone to analytical formalization, being at the very basis of rigorous kinetic theories [3]. A vast campaign of studies has been devoted, in recent years, to understand the properties of this model during the so-called homogeneous cooling state (HCS) and the linear departure from it. The system is prepared in a random homogeneous configuration with positions uniformly distributed in the box and velocities extracted from a Maxwellian with temperature $T_g(0)\equiv\langle\mathbf{v}_i^2(0)/2\rangle=1$. A thermalization phase follows, where the system evolves with elastic collisions. Finally the real inelastic evolution begins: all time and

collision counters start from this moment. During evolution, the granular temperature decreases since a fraction of kinetic energy is lost after each collision. Nevertheless the initial stage of the cooling remains homogeneous in space, with a decay of the granular temperature given by the Haff law:

$$T_g(t) = \frac{T_g(0)}{(1 + t/t_e)^2}, \tag{2}$$

with $t_e = \tau_e/\gamma$, τ_e the mean free time between collisions at the beginning of the evolution, and $\gamma = (1-\alpha^2)/4$. During the HCS, the cumulated number of collisions per particle, $\tau(t)$, grows logarithmically with time:

$$\tau(t) \propto \ln(1 + t/t_e). \tag{3}$$

In Fig. 2 we show T_g vs t (frame a) as well as τ vs t (frame b).

Simulations and linear stability analysis of macroscopic (hydrodynamiclike) models [10–12], have shown that the HCS is unstable when the size of the system L is larger than a critical size L_c. For systems large enough, therefore, spatial homogeneity is eventually broken and the formation of vortices and clusters is observed. A sign of this symmetry breaking is the departure from the Haff law: the growth of structures reduces the dissipation, reflected by a slower decay of T_g. The generally accepted scenario is a two-stage process: initially the density remains homogeneous while a macroscopic velocity field with vortical structures emerges (shear instability); after a while the density field begins to develop clusters (clustering instability). Both kinds of structures seem to obey a coarsening dynamics with characteristic lengths growing as $\sim t^{1/2}$ [12]. In Fig. 3 a sequence of snapshots of a granular gas simulation illustrates the breakdown of the homogeneous cooling state and the onset of a highly clusterized regime.

Recently the evidence of an asymptotic nonhomogeneous cooling dynamics has been shown in large ($N \sim 10^6$) event driven 2D and 3D simulations [13–16]. The observation of this "final" cooling regime has been made possible by implementing a regularization of the dynamics, in order to get rid of the inelastic collapse problem. Inelastic collapse [10] is a singularity of the inelastic hard spheres dynamics which is triggered by rare collisions happening at very low relative velocities and in situations of high density, and it is not related to the shear and clustering instability. Many kinds of regularization have been proposed: in the rest of our paper we will use the one implemented by Ben-Naim *et al.* [13], the so-called elastic cutoff: all collisions happening at a relative velocity $|(\mathbf{v}_1 - \mathbf{v}_2)\cdot\hat{\boldsymbol{\sigma}}| < v_e$ are treated as elastic. We (as well as in Ben-Naim's work) have verified that the statistics behavior (e.g., T_g and τ vs t) does not depend on the choice of v_e, provided that $v_e \ll \sqrt{T_g(t)}$. The percentage of those "fake" elastic collisions remains negligible, but they are enough to prevent the collapse.

The main characterization of the asymptotic regime, independently of the regularization mechanism, is the granular temperature decay, $T_g \sim t^{-1}$ in two dimensions. The t^{-1} law could be generally explained as the consequence of some kind of diffusion, where an energy decay $t^{-D/2}$ is expected.

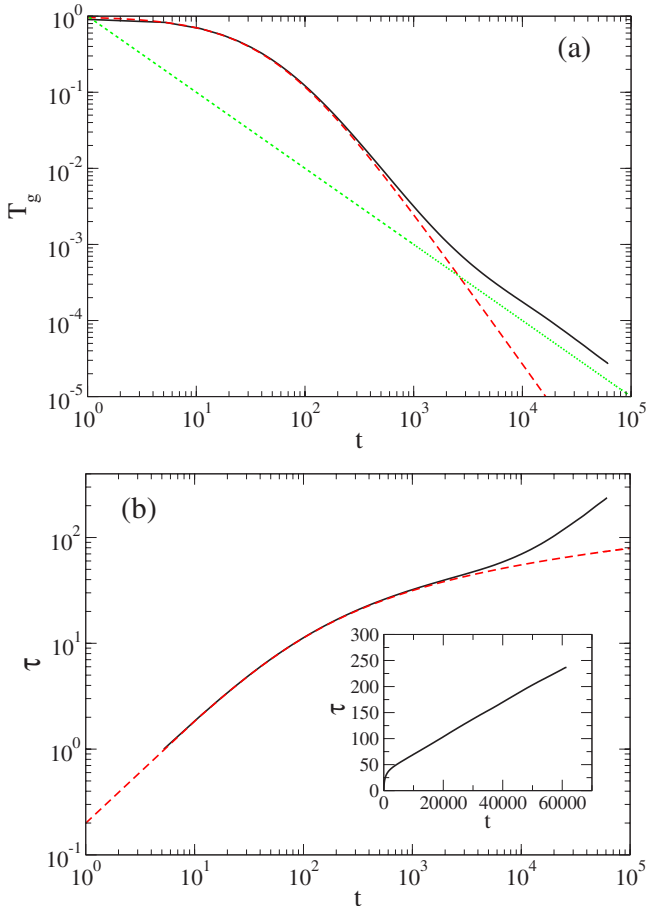

FIG. 2. (Color online) (a) Decay of granular temperature T_g vs time t. The dashed red line marks the Haff law, $T_g = 1/(1+t/t_e)^2$ with $t_e \approx 52$, the dotted green line is a t^{-1} decay. (b) Cumulated number of collisions per particle τ vs time t, the dashed red line shows the logarithmic growth of collisions in the Haff phase, $\tau = a\ln(1+t/t_e)$ with $a \approx 10$. In the inset a linear plot of τ vs t is shown, focusing on the behavior at large times ($t \gg 10^4$). The system is a gas of $N = 10^6$ inelastic hard disks with restitution coefficient $\alpha = 0.9$ in a box of size 3163×3163 (units of a diameter) with periodic boundary conditions. Averages over ten different initial conditions have been performed. Units in the figures are arbitrary, based on simulation parameters.

While this seems true for the velocity field at the beginning of the instability, i.e., still in the presence of a homogeneous density distribution [17], it becomes less evident in the asymptotic, strongly compressible, situation. Ben-Naim and coworkers have conjectured the belonging of this "final" cooling stage to the universality class of the Burgers equation: this is reasonable for a 1D inelastic gas, which is similar to a gas of sticky particles, but it has proven to be incorrect in higher dimensions [18]. A mode-coupling theory, put forward by Brito and Ernst [16], suggests an asymptotic decay of $T_g \sim \tau^{-D/2}$. While in many simulations (see, for example, the inset of the right frame in Fig. 2) the asymptotic relation between τ and t seems to be linear, this is not true for any value of α. On the contrary, the asymptotic temperature decay does not depend upon α. Isobe [14] has shown the remarkable (and unexplained) similitude between the final cooling regime and two-dimensional turbulence in incom-

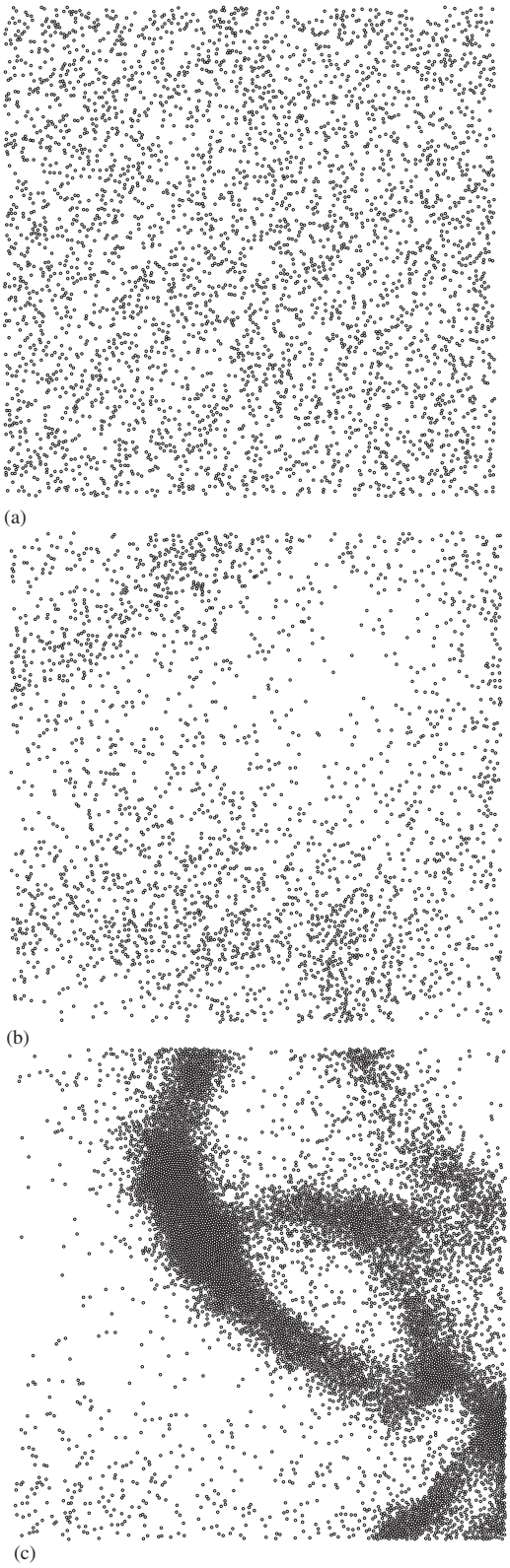

FIG. 3. Three snapshots of a small part of the gas of 10^6 inelastic hard disks with restitution coefficient $\alpha=0.9$. In the snapshots a square of surface 200×200 is portrayed, in units of a diameter, where the whole system is 3163×3163; therefore the pictures portray a fraction 0.004 of the total surface. (a) Just after thermalization [0 collisions per particle (cpp)]; (b) after 100 cpp; and (c) after 200 cpp.

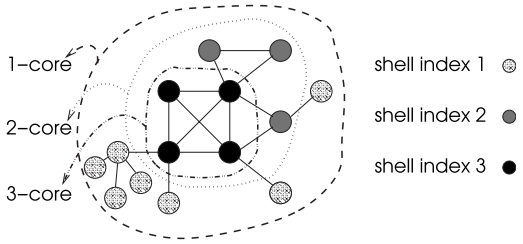

FIG. 4. This figure shows a graph and its decomposition in k-cores. The *shell index* is the maximum core that a node belongs to, then the 2-core has nodes with shell indexes 2 and 3.

pressible fluids. Miller and Luding [15], after having verified that the exponent of the algebraic decay of $T_g(t)$ is ~-1 also in $D=3$ have suggested that the formation of clusters is a sort of percolation process. Meerson and Puglisi [19] have shown that in $D=2$ elongated geometries (such that one direction is stable and the other is unstable) the HCS is followed by an intermediated *flow-by-inertia* regime, and finally a coalescence of quasisingular clusters *à la* Burgers. An observation that we report here (reserving details for further communications) is the strong narrowing of scale separation between microscopic and macroscopic dynamics, which makes a hydrodynamic description of this final cooling regime [20] difficult in practice.

III. THE NETWORK OF COLLISIONS AND THE k-CORES ANALYSIS

Let us introduce the k-core decomposition. Given a graph $G=(V,E)$ of $|V|=n$ vertices and $|E|=e$ edges, the definition from [6] of k-cores is the following.

Definition 1. A subgraph $H=(C,E|C)$ induced by the set $C\subseteq V$ is a k-core or a core of order k iff $\forall v\in C$: $\text{degree}_H(v)\geqslant k$, and H is the maximum subgraph with this property.

A k-core of G can therefore be obtained by recursively removing all the vertices of degree less than k, until all vertices in the remaining graph have degree at least k. It is worth remarking that this process is not equivalent to prune vertices of a certain degree. Indeed, a starlike subgraph with a node with a high degree that connects many vertices with degree one and connected only with a single edge to the rest of the graph is going to belong only to the first core no matter how high the degree of the node is. We will also use the following definitions.

Definition 2. A vertex i has shell index k if it belongs to the k-core but not to the $(k+1)$-core.

Definition 3. A component is a connected subgraph, i.e., a path exists between any pair of nodes in the same component.

The k-core decomposition therefore identifies progressively internal cores and decomposes the network layer by layer, revealing the structure of the different k-shells from the outmost one to the more internal one (e.g., Fig. 4).

Now, we define a collision network as follows: each particle is a node of the network, and each collision between two particles is represented by a connection between both

nodes. This network has the particularity that each node may have multiple connections with other nodes. Technically we say that a collision network is not a graph, but a multigraph, i.e., each edge may be multiple.

We have considered two possibilities to build a dynamical collision network at time t. The first is obtained collecting all collisions from time 0 to time t: we call it a *complete* network. The second one is built taking only the collisions that occurred during a window of time of fixed length (in terms of number of collisions), ending at time t: this has been called a *partial* network. Qualitatively the analysis of both networks produce the same results: the distribution of populated shells is narrow in the uncorrelated (homogeneous) phase and is very spread in the correlated (inhomogeneous) one. The shell distribution in the partial network has the advantage of being concentrated in a fixed range of shell indexes, while the complete network distribution shifts with time toward high shell numbers, since the average number of links per node is growing. On the other side, the complete network offers a better resolution of higher cores, which becomes crucial in the nonhomogeneous regime: during this regime, defining a characteristic time scale and choosing the length of the time window for the partial network gets harder and harder. For this reason, in the following, we have focused our attention on the complete network.

It is important to remark that the time complexity to compute the k-core decomposition is very low. The vertex degree d is given by the number of nearest neighbors. Given a graph G represented by its list of vertices, where each vertex has a list of neighbors, the k-core decomposition can be computed as follows.

(1) Make an ordered array of lists, where each list is composed by the vertices with the same degree. This step takes $O(n)$, where n is the number of vertices.

(2) Compute each k-core, recursively, starting by the minimum degree $d_{\min}$, until any vertex remains in the graph. The time complexity of this step is $O(e)$, where e is the number of edges.

To compute each k-core, it is enough to cut the vertices, and their corresponding edges, with a degree lower than k. Note that when a node loses a neighbor, its degree is decreased, therefore it changes its degree-list and may possibly fall into a degree-list which is being cut. Then, the final time complexity for a general graph is $O(e+n)$, which is transformed into $O(e)$ for a connected graph (where $e>n-1$).

Using this algorithm, it is very easy to compute the k-shell. Normally, the algorithm begins from the nodes in the $k-1=d_{\min}$ list. All cut vertices form the $(k-1)$-shell, while the surviving graph is the k-core. Then at each step, the k-core and the $(k-1)$-shell are obtained.

It is important to observe that a 1-core has no isolated vertices, and a 2-core has no trees. For example, given a tree T, computing its 1-core leads to the same tree T; if its 2-core is computed, the result is an empty graph. Only a graph with loops gives a nonempty 2-core. In general, a graph containing a n-clique, i.e., a graph with its n vertices all connected among themselves, has a nonempty $(n-1)$-core.

IV. RESULTS: HOMOGENEOUS SYSTEMS

In this section we present results about the analysis of the collision network in homogeneous systems. In particular we will analyze the dynamical collision network of four different models.

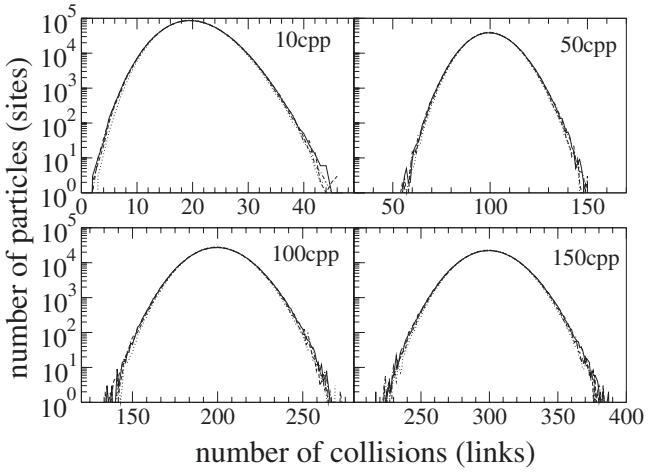

FIG. 5. Distribution of number of links per node (collisions done by each particle) at different times for the four homogeneous cases taken into account: a small inelastic system of hard disks (solid line), a gas of elastic disks (dashed line), a gas of inelastic disks simulated with the DSMC algorithm (dot-dashed line), and a randomly growing network where each link (collision) is done choosing with uniform probability over the set of all possible pairs of nodes (dotted line).

(1) A "small" system of inelastic hard disks ($\alpha=0.9$) that cools down staying in the HCS during its whole history.

(2) An elastic system ($\alpha=1$) that permanently remains homogeneous in its equilibrium dynamics.

(3) A system of inelastic hard disks simulated with the so-called homogeneous direct simulation Monte Carlo [21] (DSMC). In the homogeneous DSMC each particle can collide with any other particle (spatial coordinates are discarded) and the random choice of colliding couples is performed with a probability proportional to $(\mathbf{v}_i-\mathbf{v}_j)\cdot\hat{\boldsymbol{\sigma}}$, in order to reproduce the kernel of the collisional integral in the Boltzmann equation.

(4) A pure randomly growing network where links (collisions) are added with uniform probability on the set of all possible couples of nodes.

All four considered systems have 10^6 particles (i.e., vertices). In the first case, the size of the system is compared to the critical size given by linear stability analysis of the HCS. This analysis [12] shows that a minimum size $L_c=\frac{2\pi}{k^*}$ is needed to have unstable shear modes, with $k^*=\frac{\sqrt{1-\alpha^2}\sqrt{3}}{2\lambda}$, i.e., $L_c=\frac{4\pi\lambda}{\sqrt{1-\alpha^2}}\approx 29\lambda$, where $\lambda=L^2/(\sqrt{2}\pi N\sigma)$ is the mean free path. The small system considered here has a size $200\,000\times 200\,000$, corresponding to a density $\rho=2.5\times10^{-5}$, an area fraction 1.96×10^{-5} and a mean free path $\lambda\approx1.6\times10^4$, so that $L\sim12.5\lambda\ll L_c$. The elastic system instead has the size of the large inelastic system discussed in the next section, i.e., 3163×3163 (it is smaller in units of a diameter, but is much larger in units of a mean free path).

In Fig. 5 we present the evolution of degree distribution $f(d,\tau)$ of d edges attached to a node, with time τ measured in collisions per particle (cpp), for the four different cases. The

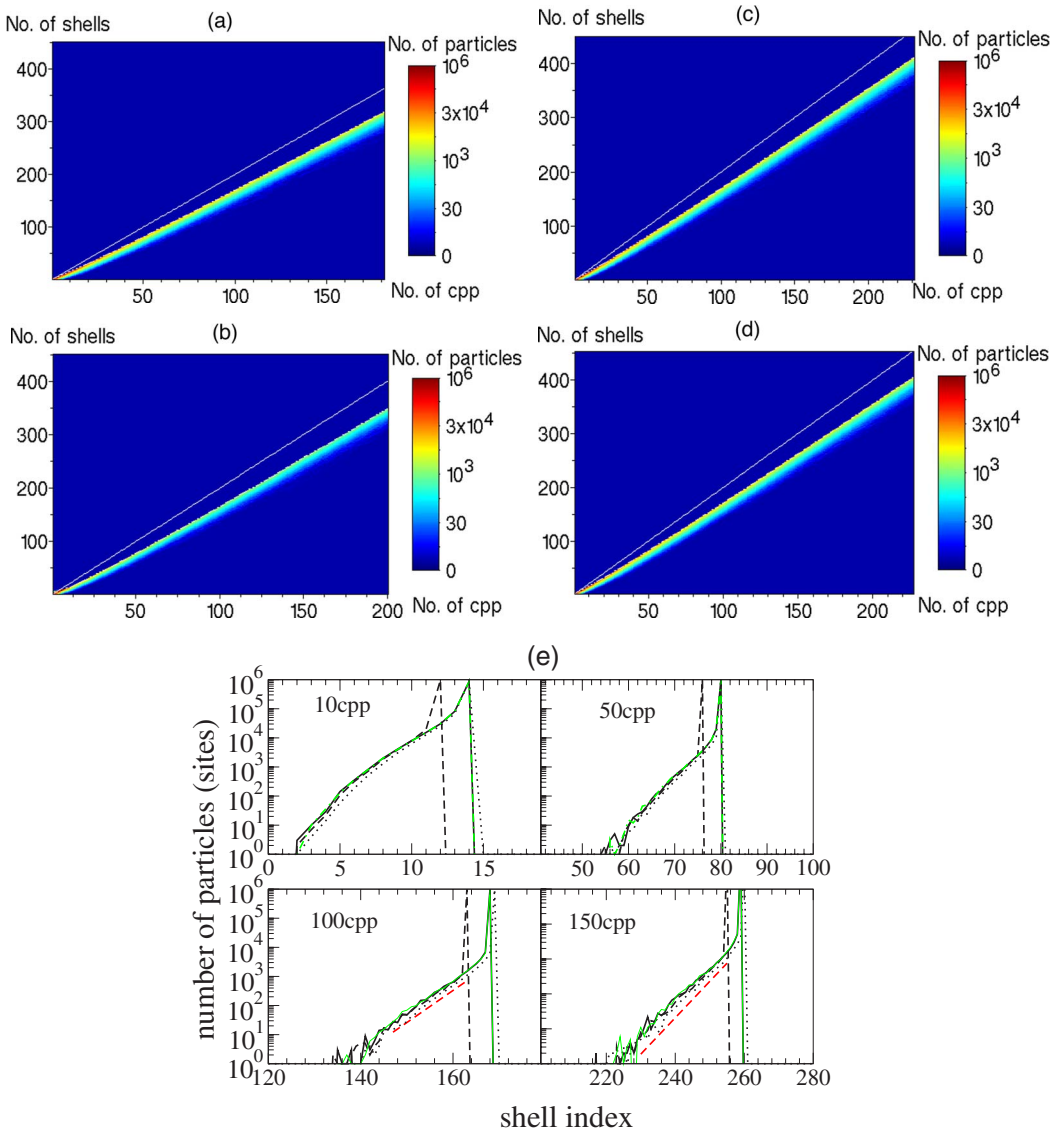

FIG. 6. (Color online) Distribution of k-shells for the four homogeneous systems against time τ measured in collisions per particle (cpp). (a)–(d) Time is on the x axis, while shell index k is on the y axis. Brightness of color indicates population (number of particles in the shell). (a) The small inelastic molecular dynamics (MD), (b) the elastic MD, (c) the DSMC, and (d) the random network. (e) Sections of the left graph at four different times: the solid line is the small system of inelastic hard disks, the dashed line is the elastic system of hard disks, the (green) dot-dashed represents the system of inelastic hard disks simulated with the DSMC algorithm, and the dotted line is the random network. The bold dashed (red) line in the two bottom graphs marks an exponential growth $\sim\exp(0.24k)$.

average number of edges attached to each vertex (i.e., of collisions done by one particle) is linearly growing with the total number of collisions, i.e., $\langle d\rangle = 2\tau$. The four systems display almost identical degree distributions. The form of the distribution is close to a Poissonian when $\langle d\rangle$ is small and becomes a Gaussian at large $\langle d\rangle$. Poissonian and Gaussian statistics are the natural expectations for homogeneous systems where no preferential attachment is at work.

In Fig. 6 results of the k-shell decomposition are shown for the four different cases. Very similar results are observed for all the cases: a small group of a few shells is populated, and the shape of the distribution is stationary and is linearly shifting in time toward high shell numbers. A shift in time is expected from the simple fact that $\langle d\rangle$ is growing. Since the shape of the distribution is conserved, we can track the growth of the average shell number looking at the index of the maximally populated shell, $k_{\max}$. We observe for all the systems a growth $k_{\max} \sim 1.8\tau \sim 0.9\langle d\rangle$. To our knowledge, the only calculation of a similar quantity is in [8], in the case of Erdös-Rényi graphs (i.e., random graphs with a Poisson degree distribution with average $\langle d\rangle$) where the largest index of a populated core grows as $0.78\langle d\rangle$. Note that even our random case is different, since we look to a random network with a *constant* total number of edges. On the other side, the shape of the shell distribution seems almost identical in all four homogeneous cases and strikingly resembles the shape of Erdös-Rényi graphs depicted in Ref. [8], with an asymmetric distribution and $k_{\max}$ coinciding with the largest index of a populated shell. In particular a nice exponential fit can be applied to the left tail of the distribution with a growth

rate that asymptotically (for large τ's) does not depend upon τ.

A core of order k can be, in principle, divided into components, i.e., each one is a connected subgraph and they are not connected among themselves. We have verified that in all four considered cases only one component is present in the graph and in all subgraphs of any core index, consistent with the scenario of the k-core percolation: the maximum core is therefore a giant fully connected component of the whole graph.

From the results of this section a first conclusion can be drawn on the properties of a dynamical collision network: lack of correlation in the process of link attachment gives place to a well-defined, narrowly peaked and shifting in time, distribution of shells. Even in the presence of inelasticity we observe an almost perfect coincidence with a randomly constructed network: this is not surprising, since the only difference (the bias coming from the collision frequency due to relative velocity) is not a preference on the degree of connection and therefore does not affect the network topology. Also the small spatial correlations present in gases of hard disks with finite diameter do not play a relevant role: at the level of diluteness, we had considered (area fraction smaller than 10%), they give place only to a small correction in the collision frequency, usually taken into account with the so-called Enskog factor in the collisional integral of the Boltzmann equation, with a small α dependence. In any case those finite diameter correlations do not bias the attachment between nodes after a given total number of collisions. Tiny discrepancies observed are, in our opinion, due to finite statistics and are not relevant.

Before proceeding, the meaning of "molecular chaos" for real finite systems can now be discussed. As mentioned in the Introduction, the only realization of a gas satisfying the true molecular chaos constraint is a gas where each particle collides with particles that are not connected (via other collisions) with its own previous history: this of course requires infinite particles and gives place to a collision network without cores of index larger than 1, i.e., a tree structure. In finite systems recollisions are always possible and they are reflected in the percolation of cores of growing indexes, as shown in this section. Anyway, a vast literature teaches us that in all systems discussed here, most of the predictions coming from kinetic equations with the assumption of molecular chaos are satisfied. As a matter of fact, the violations of molecular chaos described by the presence of cores of growing indexes are negligible for most of the physical observables. We propose, therefore, to use in this case the term "finite size molecular chaos." This assumption is analogous to the assumption, typically used in the theory of random graphs, that a graph is "locally a tree." A striking deviation from this behavior is observed when spatial homogeneity is broken, as we discuss in the next section.

V. RESULTS: NONHOMOGENEOUS COOLING

We consider here a large inelastic system breaking homogeneity (specifically spatial translational invariance). The number of particles is again 10^6. System size is 3163 $\times$3163, the density is $\rho=N/(L^2)=0.1$, corresponding to an area fraction of about 7.8% and a mean free path $\lambda \approx 4$: in this case $L \sim 790\lambda \gg L_c$. This system, after a first stage in the HCS, develops strong and persistent structures in the velocity and density field. Figure 2 clearly illustrates that after $\sim$40 cpp (collisions per particle) the HCS is no more a good description of the time evolution of energy and collision frequency. In particular, after $\sim$70 cpp, the "final" regime is reached where $T_g \sim t^{-1}$. As displayed in Fig. 3, during the whole "final" regime, a continuous condensation of clusters is at work. Visual inspection of the gas indicates the presence of groups of particles involved in a huge number of collisions dissipating a very small fraction of the energy, while the remnant particles constitute an even more dilute gas and dissipate most of the energy in collisions among themselves or against the clusters.

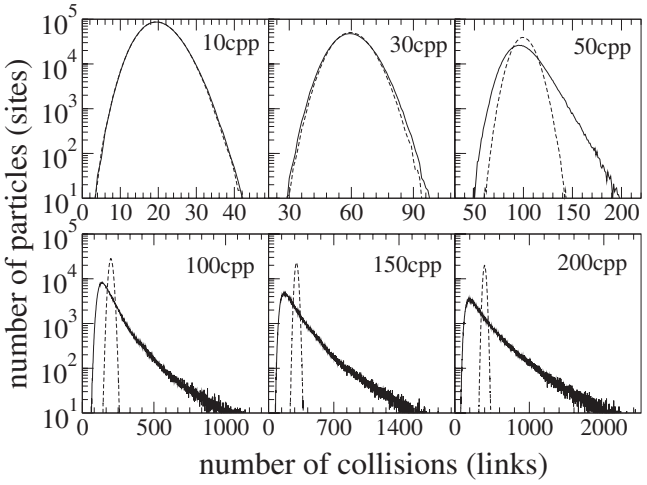

FIG. 7. Histograms of degree distribution $f(d,\tau)$ for different values of τ, i.e., of number of collisions per particle: comparison between the large inelastic system (solid line) and the elastic system (dashed line).

The analysis of degree distribution of the dynamical network is given in Fig. 7, compared to the same measure for the elastic system of the same size (which is representative of all homogeneous systems discussed previously). Degree distribution starts to deviate from the Gaussian behavior at $\sim$40 cpp, i.e., together with the departure from Haff law. The distribution develops a very fat tail at large values of the number of links per node, representing the contribution of particles trapped in clusters. No power law tails are observed, but large stretched exponentials are.

The k-core analysis of the dynamical collision network is presented, giving results averaged over ten simulations starting from different random initial conditions, in Fig. 8. Inspection of (a) of this figure reveals an immediate and striking difference with the corresponding plot for homogeneous systems in Fig. 6: at the time of deviation from the HCS ($\sim$40 cpp) given by the departure from the Haff law, the narrow distribution of populated k-shells starts to spread, while the index of the maximally populated shell begins to deviate from the linear law $k_{\max} \sim 1.8\tau$ discussed in the previous section, becoming slower. In (b), k-shell distributions at given times are shown to better illustrate the phenomenon

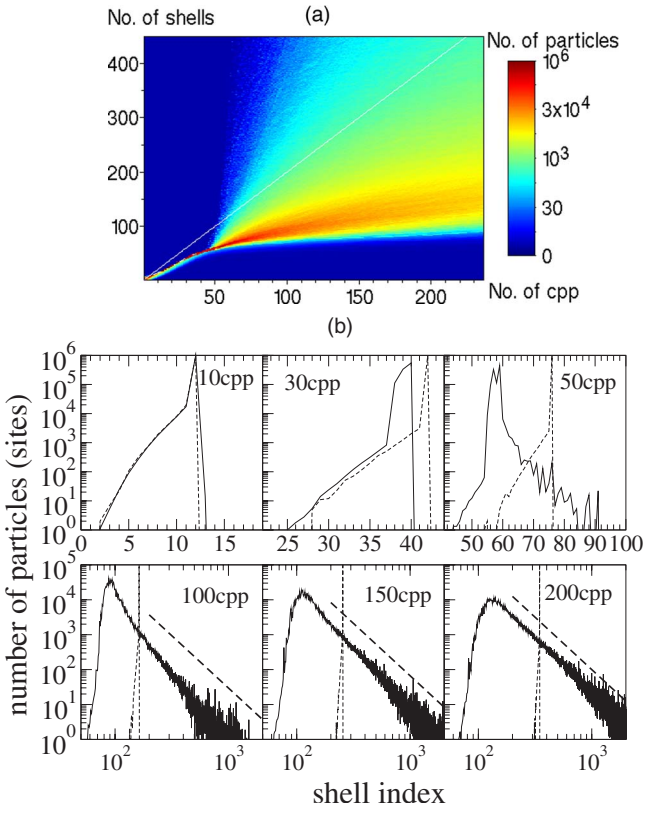

FIG. 8. (Color online) Distribution of k-shells in the large inelastic system against time τ measured in collisions per particle (cpp). (a) Time is on the x axis, while shell index k is on the y axis. Brightness of color indicates population (number of particles in the shell). The solid white line marks the 1.8τ law observed in the homogeneous case. (b) Sections of the left graph at six different times (solid line) compared with the elastic system of the same size (light dashed lines). The bold dashed line marks a power law decay with a -3 exponent.

of very large cores contagion. Shells with very high indices are populated by a consistent fraction of particles. The tail at large k's of the shell distribution is well-fitted by a power law decay with $\sim k^{-3}$, while the small and medium k ranges resemble a Gaussian function.

The analysis of connected components in the whole graphs (core of index 0) and in the core subgraphs of higher index k, shown in Fig. 9 for a given time, teach us that a large component percolates the core, but at high indexes it is accompanied by a few other lesser components. A more detailed analysis reveals that the different components are located in different spatial regions, as expected: the disconnected components represent separate clusters.

Finally in Figs. 10(a)–10(d) we display some relevant observables as a function of each shell at a given (large) time τ. The most remarkable observation concerns the average dissipated energy per collision as a function of the shell index: a strong decay (compatible with an exponential ramp) is visible. This suggests that a typical scale $k^* \sim 100-150$ (choosing a three orders of magnitude of difference), slightly depending upon τ, separates a group of shells where high dissipating collisions occur against a larger group of shells dominated by weakly dissipating collisions. This observation

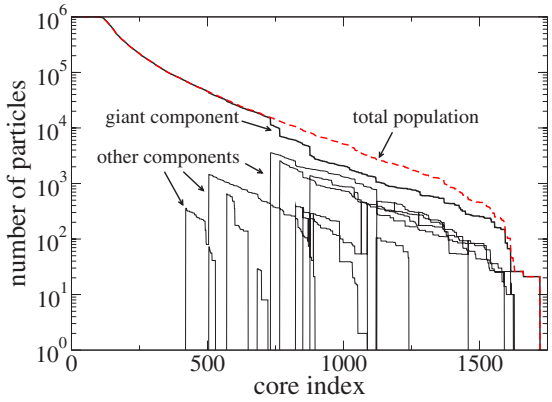

FIG. 9. (Color online) Plot of the number of particles in disconnected components in each core, as a function of the core index, at time τ=200 cpp. At small core indexes, the number of observed disconnected components is 1, then it grows up to ~6.

also provides a nice physical interpretation of k-core decomposition: such decomposition fairly manages to discriminate between the gaslike phase (few strongly dissipating collisions) and the solidlike phase (many weakly dissipating collisions).

Note that, while this separation is clear when the average dissipated energy per collision is regarded, it becomes less evident when looking at the total dissipated energy: collisions in high-index shells dissipate less energy but dominate, in number, the total number of collisions in the gas. We can still say that most of the total energy of the gas is dissipated in the first group of shells, but we cannot put a clear discriminating mark between "gas" and "solid."

Another interesting observation concerns the kinetic energy contained in the various shells. Total energy (i.e., summed over all particles in a shell) still reproduces the large peak at small shell indexes followed by a very large tail. On the other side the average kinetic energy per particle has much weaker k-dependence: all shells contain particles with similar kinetic energies, i.e., velocities in absolute value.

The spatial location of grains of a given shell index, given in the right frame of Fig. 10, confirms the above physical interpretation: particles in the first group of shells (indexes 0–150, at the time chosen) are spread in a low density-high mobility phase, while the rest of the particles constitute compact clusters: in particular, higher shell indexes individuate inner grains whose escape probabilities are smaller and smaller.

Figure 11 shows a synthetic representation of a part of the total collision network after 100 cpp (i.e., 10^8 links) for both granular molecular dynamics (MD) simulations, i.e., homogeneous [(a)–(c)] and nonhomogeneous [(d)–(f)]. Only a fraction (20%, i.e., 2×10^7) of the total number of links is considered in the construction of the picture: this leads to a distribution of shells that differs from the previous analysis (core indexes are much smaller). All particles (nodes) are placed in the graph as dots: size, gray tone (color), and position reflect various properties of that node. The gray tone (color) of a dot tells its shell index (following the scale on the right). The size represents the number of different particles linked to it (following the size scale on the left). The

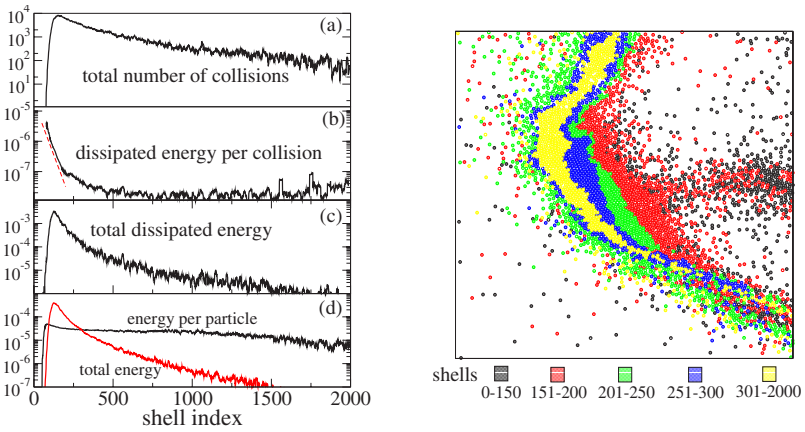

FIG. 10. (Color online) Left: statistics of physical observables in different shells at a given time (τ=200 cpp). Units are arbitrary, depending on simulation parameters. (a) Total number of collisions performed by particles in a given shell. (b) Dissipated energy per collision, together with an exponential fit of the first decay $\sim\exp(-0.03k)$. (c) Dissipated energy summed over all collisions done by particles in a given shell. (d) Average energy competing to each particle in a given shell and total energy contained in a given shell, rescaled in order to appear on the same scale. Right: a snapshot of the system at τ=200 cpp, showing in different gray tones (colors) the shell each grain belongs to.

position of each node is able to represent both its core index and the connected component (in its own core) it belongs to: each core component is a group of circles with the same center and radii proportional to the core index, while different components have displaced centers, so that they can be distinguished. Small (second order) modifications of this rule are applied to represent also the number of links of the node toward higher shells. In the visualization also a sample (only 1000) of the considered links is displayed, in order to give a flavor of the density of connections in different parts of the network. Looking, for example, at the right frame, one can clearly see that at low indexes (violet) there is only one component, at high indexes (blue-cyan) there are a few different components, while at the highest indexes (red) again only one component is present: all this is consistent with Fig. 9. The reader can find a complete description in [22,23]. From this visualization it is possible to immediately evaluate the difference between the homogeneous and inhomogeneous case. In the first case [Figs. 11(a)–11(c)] there are very few shells and most of the particles are in the maximum core, while all the cores have a unique connected component, reminding one of a random graph behavior [7]. On the contrary, in the nonhomogeneous case [frames (d)–(f) of Fig. 11], several components are present, each representing a cluster, while the index of the maximum core is much larger than in the homogeneous case.

VI. A MODEL FOR RECOLLISIONS

Here we propose a minimal algorithm to stochastically build up a network with properties similar to those observed in the collision network for homogeneous and nonhomogeneous granular gases. The number of nodes, N, is constant with time, while links connecting the pair of nodes are added in sequence. A parameter $p_{hom} \in [0,1]$ denotes the percentage of links homogeneously created. The algorithm consists of sequential steps, at each step the following happens:

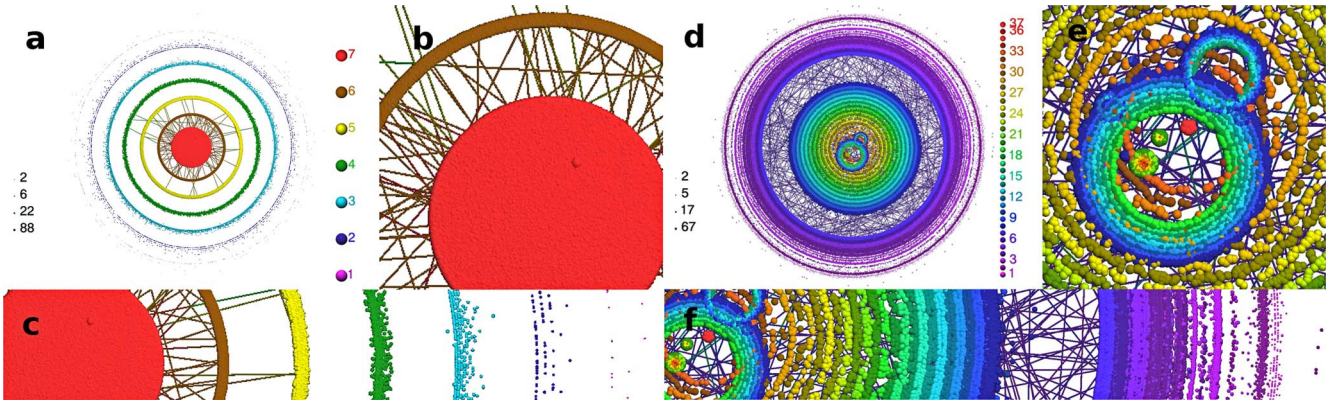

FIG. 11. (Color online) Visualization of the collision network using LaNet-vi [23]. (a)–(c) A homogeneous case, and (d)–(f) A nonhomogeneous case. Both visualizations have been done using a uniformly sampled network because of computer memory constraints (only 20% of the collisions have been taken). Each sampled network has the complete visualization [(a) and (d)], a zoom of a central part [(b) and (e)], and half of a longitudinal cut [(c) and (f)].

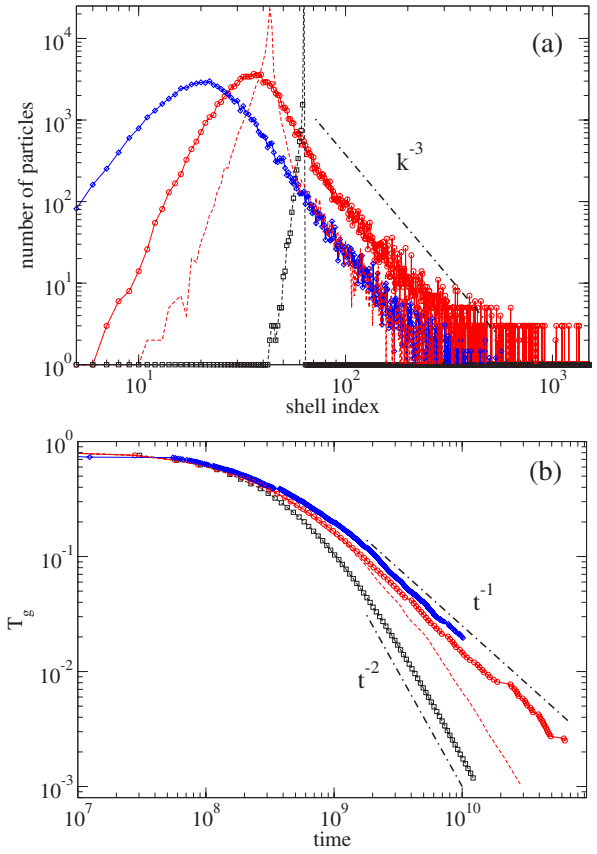

FIG. 12. (Color online) Simulations of the recollision model. (a) The number of nodes per shell, with $p_{hom}=1$ (black dashed curve with squares) after that $40N$ links have been added, $p_{hom}=0.9$ (red solid curve with circles) after that $40N$ links have been added, $p_{hom}=0.8$ (blue solid curve with diamonds) after that $25N$ links have been added, and a case (red dashed line) with $p_{hom}=0.9$ and nr chosen randomly uniformly in $[1,d_i]$, after $40N$ links. In all cases $N=10^5$. The thick dot-dashed line is a k^{-3} algebraic decay. (b) The decay of the energy in the recollision model, for the same cases. The two dot-dashed lines denote the two algebraic decays t^{-2} and t^{-1}. Here $N=10^6$ and $\alpha=0.9$. Units are arbitrary, depending on simulation parameters.

(1) The first node i is chosen with uniform probability among the N nodes;

(2) a random number x is generated in the range $[0, 1)$;

(3) if $x<p_{hom}$ the second node j is chosen with uniform probability among the $N-1$ left nodes, i.e., $j\neq i$; a new link $i-j$ is added; then repeat from 1;

(4) if $x\geqslant p_{hom}$, a sequence ("chain of recollisions") of nr links is added; nr is equal to the degree d_i of node i (number of links attached to i);

For 1 to nr do the following:

(i) Choose uniformly one of i's links, and put another link to that neighbor;

(ii) when the sequence of nr "recollisions" ends, repeat from 1.

The results of the simulations of this simple model appear in Fig. 12(a). When $p_{hom}=1$, the results of all homogeneous models are reproduced. The distribution of shells is peaked at a value $\sim 0.88\langle d\rangle$ and all populated cores are spanned by a single connected component. When $p_{hom}<1$, the situation radically changes: the distribution of shells becomes broad, fairly resembling those of Fig. 8, with many components in the cores with high indexes. In particular the Gaussian-like shape in the low-index range and k^{-3} power law decay for the population of shell with high indexes is reproduced. These remarkable findings suggest that the above algorithm contains the ingredients sufficient to explain the topology of recollisions in nonhomogeneous granular gases. We have also tempted different algorithms, changing the kind of preferential bias: most of them generated strongly different distributions. A variant of the model where nr is uniformly randomly chosen between 1 and d_i displays an intermediate behavior, with a peak at low-index shells, characteristic of the homogeneous systems, and the k^{-3} tail observed in correlated systems. In summary, the mechanism depicted in the rules (1)–(4) above seems the only one to fully recover the physical distribution of shells and components.

To conclude this analysis, we now speculate about the possibility of recovering the physical decay of the granular temperature using this minimal model for recollisions. Assigning initial random velocity vectors (in 2D) to all N nodes, from a normal distribution, and updating the velocities of linked nodes i and j by Eq. (1) at every new link, we obtain a decay of granular temperature. In the collision rule we randomly choose the angle (with a fixed axis) of the unitary vector $\hat{\boldsymbol{\sigma}}$ from a uniform probability in $[0,2\pi)$. Our first observation concerns energy dissipation: as in the granular gas [see Fig. 10(b)], lower shells contain the most dissipating collisions. One can also study energy dissipation in different kinds of collisions (those with $x<p_{hom}$ against those with $x\geqslant p_{hom}$): on average, taken over a large and fixed number of total collisions, the energy dissipated in the first kind is two orders of magnitude larger than the second.

Finally, we have provided our network model with a physical time t: at each new link (collision), time advances of a step $dt=1/|(\mathbf{v}_i-\mathbf{v}_j)\cdot\hat{\boldsymbol{\sigma}}|$. This allows us to measure the time decay of temperature $T_g(t)$, which is displayed in Fig. 12(b). One can easily recognize the Haff decay $T_g\sim t^{-2}$ in the homogeneous situation, $p_{hom}=1$, i.e., in the absence of recollisions chains, and the nonhomogeneous decay t^{-1} when $p_{hom}<1$. The consistency of the $p_{hom}=1$ case with the Haff law is expected since, for this choice of the parameter, the model is equivalent to the DSMC model discussed as the third case in Sec. IV: particles in fact collide at random, but their collision rate is proportional $1/dt\equiv|(\mathbf{v}_i-\mathbf{v}_j)\cdot\hat{\boldsymbol{\sigma}}|$. Note also that the variation with nr random in $[1,d_i]$ does not reproduce the t^{-1} decay when $p_{hom}<1$. The same happens, for example, if one takes nr to be a fixed fraction of d_i. Since the k^{-3} tail is obtained also with those variations of the model, we must conclude that the t^{-1} energy decay is much less related to such a tail than to the shape of shell distribution of low indexes. This is consistent with the observation that energy dissipation is mostly concentrated in the low index range.

These are preliminary results that are being explored in an ongoing investigation [24]. Nevertheless, already at this level, they are striking and indicate that the proposed recollision mechanism is close to the one at work in the asymptotic nonhomogeneous state of the granular gas.

VII. CONCLUSIONS

In this work we have exploited a statistical method, originally introduced in the theory of random graphs, to gather information about recollisions (i.e., collisions among correlated particles) in a cooling granular gas. We constructed a network using the collision sequence up to a given time, then we decomposed it in the k-core and k-shell structure. In the homogeneous state, the finiteness of the system naturally induces a giant component that percolates the core of index $k_{\max} \sim 1.8\tau$ where τ is time measured as a number of collisions per particles. When the gas becomes inhomogeneous, because of inelasticity and large size, the system separates into two populations with dramatically different core statistics: a large component percolates the low index k-cores, while the rest of the gas (a non-negligible part) is found in a finite (small) number of disconnected components at very high index k-cores, corresponding to spatial clusters. The dilute low-core phase is characterized by strongly dissipating collisions, while in the clustered high-core phase the dissipated energy per collision is ~ 100 times smaller.

The whole phenomenology is well-reproduced by a simple model which distillates the crucial ingredients of the recollision mechanism. This model consists of a randomly growing network which, tuning a "homogeneity" parameter, displays the same features of both homogeneous and nonhomogeneous granular gases. The success of this model is the ability to reproduce, when supplied with a reasonable measure of physical time, the observed decay of temperature $T_g \sim t^{-1}$ which has received many nonconclusive interpretations in the previous literature [13,15,16]. The lack of spatial coordinates for particles, in the proposed algorithm, suggests that the statistics of recollisions and the energy decay do not directly depend on the spatial arrangement of clusters, which is usually observed to happen in the form of stringlike structures.

The collision network analysis can also be applied to any "hard core" system, including systems with soft interactions that can be simplified as piecewise hardlike potentials. A natural extension is the study of hard disks and spheres gases at very high packing fractions, with the hope of elucidating the glass transition in off-lattice systems, as well as experimental studies of granular materials, where the use of rapid cameras is today able to collect huge amounts of collisional data.

ACKNOWLEDGMENTS

The authors wish to thank the Laboratoire de Physique Théorique d'Orsay, at the University of Paris-Sud, for hospitality and CPU time. J.I.A.H. acknowledges the support of European Commission, Contract No. 001907 (DELIS). A.P. acknowledges the support of the European Commission Grant No. MERG-021847. The work of A.P. has also been supported by the EU under RD Contract No. IST-1940 (ECAgents).

[1] L. P. Kadanoff, Rev. Mod. Phys. **71**, 435 (1999).
[2] P. G. Debenedetti and F. H. Stillinger, Nature (London) **410**, 259 (2001).
[3] *Granular Gases*, edited by T. Pöschel and S. Luding, Lecture Notes in Physics, Vol. 564 (Springer, Berlin, 2001).
[4] I. Goldhirsch, Chaos **9**, 659 (1999).
[5] A. Puglisi, F. Cecconi, and A. Vulpiani, J. Phys.: Condens. Matter **17**, S2715 (2005).
[6] V. Batagelj and M. Zaversnik, e-print arXiv:cs.DS/0202039.
[7] J. I. Alvarez-Hamelin, L. Dall'Asta, A. Barrat, and A. Vespignani, e-print cs.NL/0504107.
[8] S. N. Dorogovtsev, A. V. Goltsev, and J. F. F. Mendes, Phys. Rev. Lett. **96**, 040601 (2006); A. V. Goltsev, S. N. Dorogovtsev, and J. F. F. Mendes, Phys. Rev. E **73**, 056101 (2006).
[9] C. Toninelli, G. Biroli, and D. S. Fisher, Phys. Rev. Lett. **96**, 035702 (2006); M. Sellitto, G. Biroli, and C. Toninelli, Europhys. Lett. **69**, 496 (2005); J. M. Schwarz, A. J. Liu, and L. Q. Chayes, Europhys. Lett. **73**, 560 (
[10] S. McNamara and W. R. Young, *ibid.* **4**, 496 (1992); Phys. Rev. E **50**, R28 (1994).
[11] I. Goldhirsch and G. Zanetti, Phys. Rev. Lett. **70**, 1619 (1993).
[12] T. P. C. van Noije, M. H. Ernst, R. Brito, and J. A. G. Orza, Phys. Rev. Lett. **79**, 411 (1997).
[13] E. Ben-Naim, S. Y. Chen, G. D. Doolen, and S. Redner, Phys. Rev. Lett. **83**, 4069 (1999); X. Nie, E. Ben-Naim, and S. Chen, *ibid.* **89**, 204301 (2002).
[14] M. Isobe, Phys. Rev. E **68**, 040301(R) (2003).
[15] S. Miller and S. Luding, Phys. Rev. E **69**, 031305 (2004).
[16] R. Brito and M. H. Ernst, Europhys. Lett. **43**, 497 (1998).
[17] A. Baldassarri, U. M. Marconi, and A. Puglisi, Europhys. Lett. **58**, 14 (2002); Phys. Rev. E **65**, 051301 (2002).
[18] E. Trizac and A. Barrat, Eur. Phys. J. E **3**, 291 (2000).
[19] B. Meerson and A. Puglisi, Europhys. Lett. **70**, 478 (2005).
[20] B. Meerson and A. Puglisi (unpublished).
[21] G. A. Bird, *Molecular Gas Dynamics and the Direct Simulation of Gas Flows* (Clarendon, Oxford, 2004); M. J. Montanero and A. Santos, Granular Matter **2**, 53 (2000).
[22] J. I. Alvarez-Hamelin, L. Dall'Asta, A. Barrat, and A. Vespignani, in *Proceedings of Advances in Neural Information Processing Systems* (MIT Press, Cambridge, 2006), Vol. 18, pp. 41–50.
[23] Large Network visualization tool, see URL http://xavier.informatics.indiana.edu/lanet-vi/
[24] J. I. Alvarez-Hamelin and A. Puglisi (unpublished).